

Electrical Conductivity and Permittivity of Murine Myocardium

Karthik Raghavan, John E. Porterfield, Anil T. G. Kottam, Marc D. Feldman, Daniel Escobedo, Jonathan W. Valvano, *Member, IEEE*, and John A. Pearce*, *Senior Member, IEEE*

Abstract—A classic problem in traditional conductance measurement of left ventricular (LV) volume is the separation of the contributions of myocardium from blood. Measurement of both the magnitude and the phase of admittance allow estimation of the time-varying myocardial contribution, which provides a substantial improvement by eliminating the need for hypertonic saline injection. We present *in vivo* epicardial surface probe measurements of electrical properties in murine myocardium using two different techniques (a digital and an analog approach). These methods exploit the capacitive properties of the myocardium, and both methods yield similar results. The relative permittivity varies from approximately 100 000 at 2 kHz to approximately 5000 at 50 kHz. The electrical conductivity is approximately constant at 0.16 S/m over the same frequency range. These values can be used to estimate and eliminate the time-varying myocardial contribution from the combined signal obtained in LV conductance catheter measurements, thus yielding the blood contribution alone. To study the effects of albumin on the blood conductivity, we also present electrical conductivity estimates of murine blood with and without typical administrations of albumin during the experiment. The blood conductivity is significantly altered ($p < 0.0001$) by administering albumin (0.941 S/m with albumin, 0.478 S/m without albumin).

Index Terms—Admittance, blood conductivity, conductance, myocardial conductivity, myocardial permittivity.

I. INTRODUCTION

DETERMINATION of left ventricular (LV) pressure–volume (P – V) relations has provided a framework for understanding cardiac mechanics in larger experimental animals and humans [1]. Extension of this technique to the mouse model has proven valuable [2]. Determination of instantaneous volume in the murine LV is difficult due to the small heart size

Manuscript received April 23, 2008; revised September 12, 2008. Current version published July 15, 2009. This work was supported in part by the National Institutes of Health under Grant R21 HL079926 and a U.S. Department of Veterans Affairs (VA) Merit Grant (MDF). *Asterisk indicates corresponding author.*

K. Raghavan, J. E. Porterfield, and J. W. Valvano are with the Department of Electrical and Computer Engineering, The University of Texas at Austin, Austin, TX 78712 USA (e-mail: karthikraghavan@mail.utexas.edu; john.porterfield@mail.utexas.edu; valvano@mail.utexas.edu).

A. T. G. Kottam was with the Department of Biomedical Engineering, The University of Texas at Austin, Austin, TX 78712 USA. He is now with Scisense, Inc., London, ON N6E 3A1, Canada (e-mail: akottam@scisense.com).

M. D. Feldman and D. Escobedo are with the Department of Medicine, The University of Texas Health Sciences Center at San Antonio, San Antonio, TX 78229 USA (e-mail: feldmanm@uthscsa.edu; escobedod@uthscsa.edu).

*J. A. Pearce is with the Department of Electrical and Computer Engineering, The University of Texas at Austin, Austin, TX 78712 USA (e-mail: jpearce@mail.utexas.edu).

Color versions of one or more of the figures in this paper are available online at <http://ieeexplore.ieee.org>.

Digital Object Identifier 10.1109/TBME.2009.2012401

(5 mm length, 160 mg mass, and 40 μ L LV volume) and its rapid heart rate (500–700 beats/min). Approaches such as ultrasonic crystals [2], MRI [3], [4], and echocardiography [4] have been used to measure instantaneous LV volume with some degree of success. Unfortunately, all these technologies have severe limitations, particularly during dynamic maneuvers, such as transient occlusion of the inferior vena cava or aorta, which are required to generate load-independent indexes of contractility.

Conductance catheter technology, as introduced by Baan *et al.* in 1981 [6], offers a more robust alternative to generate instantaneous LV P – V relations in the intact murine heart. Single-frequency conductance has been used in mice to generate measures of ventricular function [5], [7], [8]. However, the traditional conductance method is limited in the mouse because the instantaneous LV conductance signal includes both blood conductance and parallel admittance in the myocardium and, unless corrected, yields an overestimate of the true LV blood volume [6]. Investigators have applied the hypertonic saline technique developed for larger mammals to determine a single value of steady-state parallel (cardiac muscle) conductance and used it for the derivation of absolute LV volume [9]. The saline technique, however, is problematic in small animals such as mice and rats since administration of even small volumes of hypertonic saline significantly alters both blood resistivity and hemodynamics (i.e., blood volume) [5], violating the framework of the governing assumptions [6]. Simultaneous measurement at two frequencies combined with the hypertonic saline technique has been proposed by other investigators [10]–[12]. However, in all cases, these methods determine only a single value of steady-state parallel conductance. Thus, conductance measurement in its present reduction to practice, in both small and large subjects, cannot calculate the instantaneous change in parallel conductance occurring throughout the cardiac cycle as the LV cavity shrinks around the intracardiac electric field during occlusion of the inferior vena cava or at end systole.

Measurements of the permittivity of muscle by Gabriel *et al.* [13], [14] suggest that the relative permittivity of cardiac muscle exceeds 15 000 at 20 kHz. We hypothesize that the electric permittivity of muscle *in vivo* is so high that the admittance in the LV at frequencies in this range can be used to identify and separate the cardiac muscle component from the combined admittance measurement. The fundamental observation is that blood is semiconducting, over the same frequency range, so all frequency-dependent admittance is due to the muscle component only, i.e., for a tetrapolar catheter in the LV, the admittance consists of two parallel components from blood and

myocardium:

$$Y_{\text{meas}} = Y_b + Y_m = G_b + G_m + j\omega C_m \quad (1)$$

where Y is admittance (in siemens), G is conductance (in siemens), ω is the angular frequency (in radians per second), C is capacitance (in farads), “meas” refers to the measured signal, “b” to the blood alone, and “m” to the myocardium.

For any electric field spatial distribution E in a homogeneous medium

$$G = \frac{I}{V} = \sigma \frac{\iint E \cdot dA}{-\int E \cdot dl} = \sigma F \quad (2a)$$

$$C = \frac{Q}{V} = \varepsilon \frac{\iint E \cdot dA}{-\int E \cdot dl} = \varepsilon F \quad (2b)$$

where I is the current (in amperes), V the potential (in volts), σ the electrical conductivity (in siemens per meter), Q the charge (in coulombs), ε the electric permittivity (in farads per meter), and F is the electric field form factor, or “cell constant,” common to both relations (in meters). The symmetry in the relationships of (2a) and (2b) leads to the familiar “conductance–capacitance” analogy. The symmetry is also the feature that allows identification and elimination of the cardiac muscle from the combined admittance signal: if C_m is measured, then G_m can be calculated

$$G_m = C_m \frac{\sigma_m}{\varepsilon_m}. \quad (2c)$$

An accurate value for the σ_m/ε_m ratio is required to apply this new method for eliminating the parallel admittance of cardiac muscle.

The dominant trend in the literature [15]–[21] following the original form of Baan *et al.*'s equation [6] is to express the electrical properties in the form of resistivity. However, when the tetrapolar catheter is placed in the LV, the current path through the myocardium flows essentially in parallel with the current path through the blood. Therefore, it is substantially more convenient to express the electrical properties in the form of electrical admittivity rather than impedivity. This is because over the frequency range of interest, the admittance of (1) describes the electrical behavior of the cardiac muscle very well, and admittances in parallel add simply rather than combine hyperbolically as do parallel impedances. Complex admittivity (ψ) has been used in impedance tomography research [23], [24] and is the formulation of choice over complex resistivity.

Equation (1) describes the admittance relationship when a catheter is placed within the LV of the heart. This relationship involves contributions from both the blood and the myocardium. However, this equation modifies into a simpler form when a surface probe is placed on the epicardium to measure the properties of the myocardium alone

$$Y_m = G_m + j\omega C_m. \quad (3a)$$

Thus, the measured myocardial admittivity ψ_m (in siemens per meter) is

$$\psi_m = \frac{Y_m}{F} = \frac{G_m + j\omega C_m}{F} = \sigma_m + j\omega\varepsilon_m \quad (3b)$$

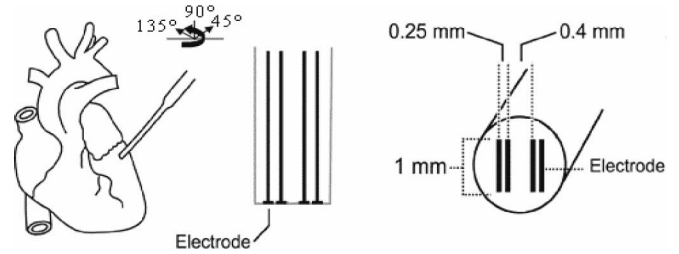


Fig. 1. Epicardial admittivity surface probe consists of 1-mm-long four electrodes spaced at 0.25 mm (typical) and 0.4 mm center to center between electrodes 2 and 3. Suction ports permit application of a mild vacuum to assist in securing the electrode.

where Y_m is the admittance of the myocardium (in siemens), and F is the cell constant described in (2a) and (2b). This definition for admittivity is clearly harmonious with Ampere’s law in point form

$$\nabla \times \mathbf{H} = \mathbf{J} + j\omega\mathbf{D} = (\sigma + j\omega\varepsilon) \mathbf{E} = \psi\mathbf{E}. \quad (4)$$

II. METHODS

In this study, we measure the electrical properties of the murine myocardium (permittivity ε_m and conductivity σ_m) in order to estimate and eliminate the myocardial contribution [Y_m , (3a)] from the combined contribution [Y_{meas} , (1)] in the LV, thus yielding the blood contribution alone in real time throughout the cardiac cycle.

A. Epicardial Surface Probe

A miniature tetrapolar surface probe was applied to the epicardial surface of the beating murine heart *in vivo* (Fig. 1). It was custom-fabricated to our specifications by The University of Texas Health Science Center at San Antonio (UTHSCSA), San Antonio. The probe contains four parallel platinum electrodes aligned with an intraelectrode spacing of 0.25, 0.4, and 0.25 mm between electrodes 1 and 2, 2 and 3, and 3 and 4, respectively. In the standard tetrapolar technique, electrodes 1 and 4 are driven with a current source and electrodes 2 and 3 are used for potential measurement at negligible current (due to the high input impedance of the voltage sensing differential amplifier). The tetrapolar method is thus essentially insensitive to the series electrode–electrolyte interface impedance of the measurement electrodes.

The electrode design was modeled after an electrode developed for the canine heart by Steendijk *et al.* [15]. However, their electrode spacing was designed to sample only the epicardium. We used effectively wider electrode spacings relative to the myocardial thickness to gain a greater depth of penetration by the electric field. This minimizes the effect of tissue anisotropy in the “longitudinal plane,” as it were, by measuring over a substantial fraction of the ventricular free wall thickness. Consequently, the effect of anisotropy due to fiber orientation within layers of myocardium is averaged. The substantial anisotropy between longitudinal (to the fiber) and transverse measurements is not addressed by this approach. In a parallel study [24], it was confirmed (by measurement at four different orientations of 0°,

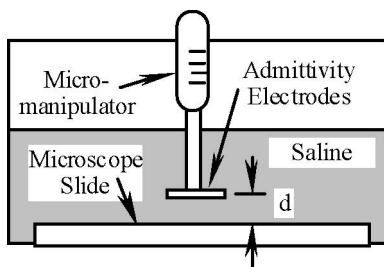


Fig. 2. Experimental setup to measure field penetration depth of surface catheters [25], [26].

45°, 90°, and 135°) that probe orientation effects showed no variation more significant than intrameasurement and interanimal variability.

B. Surface Probe Depth of Penetration

The effective measuring depth of the surface probe (Fig. 1) was determined experimentally in a saline bath by advancing the probe normally toward an insulating glass surface with a micromanipulator (Fig. 2). The “effective depth” was defined as the depth at which the measured conductance decreased 5% from the value at large depth [25], [26].

This measurement determines the thickness of myocardium at which a substrate material affects the probe current field sufficiently to be reflected as a measurable change at the voltage electrodes. Separate finite-element method (FEM) numerical studies (not included here) confirm that the effective depth over an insulator is essentially the same as the effective depth over a blood substrate.

C. Instrumentation

Three different sets of measurements at frequencies of 2, 5, 10, 20, and 50 kHz are compared in this study. The first one measures only the magnitude of the admittance signal at different frequencies. (This is termed the “conductance” approach in this study.) The next two measurement techniques involve complex measurement (both magnitude and phase) of the admittance using two different approaches: the “digital” and “analog” approaches to distinguish the two admittance measurement techniques.

1) *Conductance Measurements (Admittance Magnitude Only)*: The admittance magnitude measurement system is diagrammed in Fig. 3(a). A function generator board (Data Translation, Inc., Marlboro, MA) was used to produce sinusoidal voltages at the desired excitation frequency. The function generator output was converted into a current signal (10 μ A rms) that was applied to the two outer electrodes, 1 and 4 in Fig. 1. The instantaneous voltage signal between the inner electrodes, 2 and 3 in Fig. 1, was: 1) amplified with an instrumentation amplifier (AD624, Analog Devices, Norwood, MA); 2) rectified and inverted with a divider chip (MPY100, Texas Instruments Incorporated, Dallas, TX); and 3) scaled to +5 V to represent the conductance signal over the range of expected values. The output was sampled at a sampling rate of 1 kHz using Power-

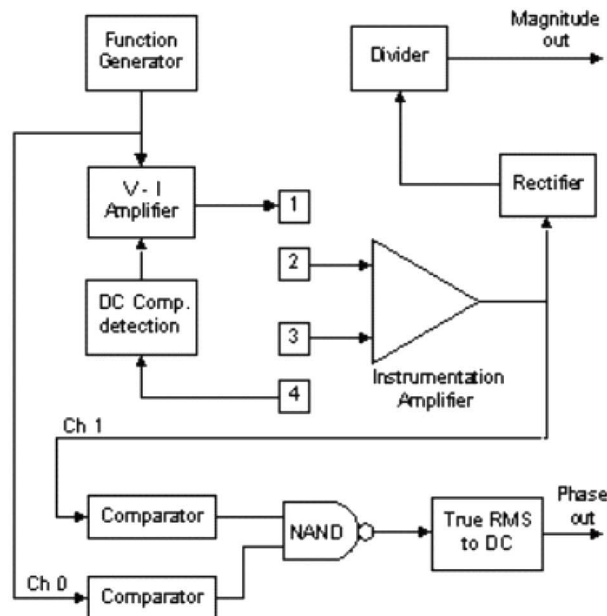
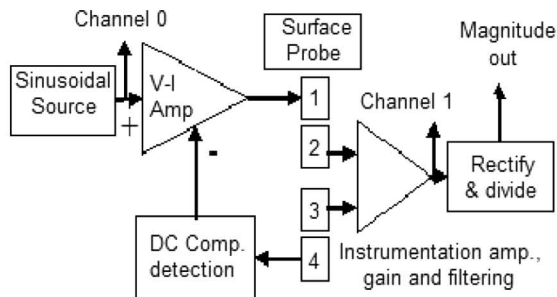


Fig. 3. (a) Block diagram of instrumentation used for admittance measurements. The magnitude output is the rectified dc amplitude signal. (b) Block diagram of instrumentation used for complex plane (magnitude and phase) admittance measurements (analog method) [28], [29].

lab (AD Instruments Pty Ltd., Bella Vista, N.S.W., Australia) data acquisition hardware and analyzed using Chart Acquisition Software (AD Instruments Pty Ltd.).

2) *Admittance Magnitude and Phase Measurement by the Digital Method*: In this technique, the reference voltage was sampled at the input to the current source, marked as “Channel 0” in Fig. 3(a). The output voltage was measured and sampled just prior to the rectification stage, marked as “Channel 1” in Fig. 3(a). The data channels were simultaneously sampled at 5 million samples per second, with a 12-bit data acquisition card (Model: NI PCI-6110, National Instruments, Austin, TX) on the Peripheral Component Interconnect (PCI) bus of the computer. For frequencies less than 5 kHz, a continuous data epoch comprised 10 000 samples (2 ms of data, four cycles at 2 kHz), and for frequencies of 5 kHz or greater, an epoch comprised 1000 samples (200 μ s of data, or one cycle at 5 kHz). At each frequency, 100 data epochs were collected and analyzed over a period of approximately 4 s by fast Fourier transform in a LabVIEW program (National Instruments) written for the purpose to determine the phase angle. This was repeated five times for

each mouse in the study, and the 500 estimates of the phase angle were combined with magnitude information to estimate the mean and standard deviation of the electrical conductivity and permittivity in a MATLAB program (The Mathworks, Inc., Natick, MA)— $N = 500$ at each frequency [27], [28].

3) *Admittance Magnitude and Phase Measurement by the Analog Method:* The “analog” technique measures admittance magnitude and phase in hardware. This instrument is described by Kottam [29], and Fig. 3(b) is a block diagram for this instrument. The phase difference is determined using the reference voltage signal and the filtered output voltage signal. These signals are converted to square waves and applied through NAND logic to generate pulses whose duty cycle varies according to the phase difference between the signals. The relative duty cycle is converted to a dc signal using a true rms detector [29]. This instrument has a sensitivity of 100 mV° for the phase measurement.

Simultaneous admittance magnitude and phase measurements were made using this device in real time. The outputs were sampled at a sampling rate of 1 kHz and acquired using Powerlab.

D. Calibration

Calibration of the conductance (magnitude of admittance) measurement device was accomplished with 1% metal film resistors between 267Ω ($3750 \mu\text{S}$) and $5.33 \text{ k}\Omega$ ($188 \mu\text{S}$). The calibration resistors were tested on an Agilent, Inc., Model 4194A Impedance/Gain-Phase Analyzer to ensure that no inductive or capacitive behavior was observable in them over the frequency range of interest, 2–50 kHz. This method was employed for the calibration of the magnitude of admittance of all three instruments mentioned before.

The small epicardial surface probe cable has substantial interwire capacitance: there are six interelectrode parallel capacitances among the four lead wires. The net effect of these capacitances was studied using a relatively large volume of saline of known electrical conductivity. Different conductivity saline solutions were prepared in the range of $800\text{--}10\,200 \mu\text{S}/\text{cm}$, or $0.08\text{--}1.02 \text{ S}/\text{m}$ at 37°C . This range of conductivities includes the range of effective conductivities of blood and myocardium. The conductivity of the saline solutions was measured with a Hanna Model HI 8033 conductivity meter (Hanna Instruments, Woonsocket, RI). The saline solutions were placed in large beakers, and the epicardial surface probe was advanced just enough to touch the surface of the saline solution. Admittance magnitude and phase measurements were made using both the digital and analog admittance instruments. Calibration curves (measured admittance phase versus conductivity) were constructed at each measurement frequency. Fig. 4 is a representative sample saline calibration curve performed with the epicardial surface probe using the digital method. Because saline is semiconducting, the phase responses in Fig. 4 occur only because of the capacitances of the lead wires. The net effect of these capacitances was compensated by this calibration.

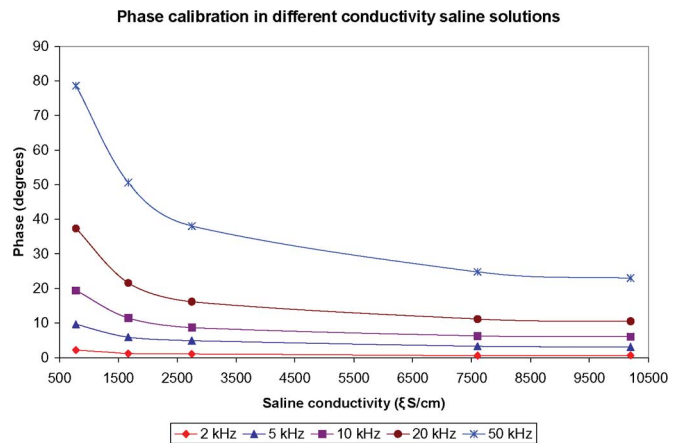


Fig. 4. Sample saline calibration curves measured using the digital method. The graph shows measured admittance phase as a function of saline conductivity for various frequencies. These curves would be used in the estimation of myocardial electrical properties to calibrate the capacitance of the epicardial probe [26].

E. Murine Studies

The Institutional Animal Care and Use Committee (IACUC) at The UTHSCSA and at The University of Texas at Austin approved all experiments. A total of 80 mice were studied by magnitude measurements: CD-1 mice ($N = 33$), BKS.Cg-m + / + Lepr^{db} (*db/db*) diabetic mice ($N = 15$), as well as their nondiabetic littermates, and C57BlkS (*db/+* or *+/+*, $N = 15$) aged 8–11 weeks were used. Ten additional CD-1 mice were studied by the digital admittance magnitude and phase measurements. Seven additional C57BlkS mice were studied by the analog admittance magnitude and phase measurement.

Mice were anesthetized by administration of urethane ($1000 \text{ mg}/\text{kg}$ i.p.) and etomidate ($25 \text{ mg}/\text{kg}$ i.p.), and mechanically ventilated with a rodent ventilator set at 150 breaths/min ($100\% \text{ O}_2$). Mice were placed on a heated, temperature-controlled operating table for small animals (Vestavia Scientific, Birmingham, AL). Experiments were performed at a murine body temperature of 37°C . The chest was entered via an anterior thoracotomy. The tetrapolar surface probe, mounted on a micromanipulator, was placed on the LV epicardium of the intact beating mouse heart. We verified that the surface probe made complete contact with the myocardium by checking the quality of the signal.

F. Blood Conductivity Studies

The purpose of this experiment was to study the electrical properties of murine blood. This study was extended to examine the effects of albumin on the electrical conductivity measurements of murine blood, since albumin is often administered by researchers to obtain physiologic blood pressures in murine studies.

Previous studies by Reyes *et al.* have shown that murine blood conductivity is not significantly different between different strains of mice [24]. Albumin (0.4 mL volume per mouse)

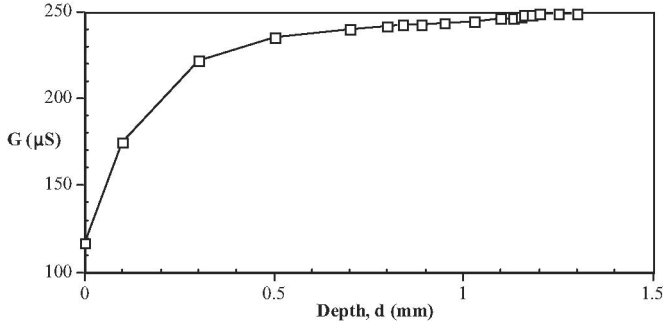


Fig. 5. Experimental measurements of the effective measurement depth of the surface probe.

was administered to the C57BlkS mice but not to the CD-1 mice to examine this variable. At the end of the *in vivo* studies, blood was collected from the LV of the mouse and placed into a plastic vial (2 mL volume). The surface probe was advanced normal to the surface until complete contact with the blood surface was made. Admittance magnitude and phase estimations were performed at the same frequencies as for the epicardial studies.

III. RESULTS

A. Surface Probe Effective Depth

In Fig. 5, the measured response at large depth is 249 μS , which decreases to 237 μS at a depth of 0.6 mm. The 0.6 mm effective depth is less than the average thickness of the murine myocardium in the LV free wall—approximately 1.2 mm at end systole and 0.8 mm at end diastole.

Blood is approximately four times more conductive than cardiac muscle—around 0.5 S/m compared to a range of 0.11–0.17 S/m, respectively [24]. As mentioned, numerical models show that the effective depth over an insulator is essentially the same as over a blood substrate (i.e., within 15%). Therefore, the surface probe measurement is not significantly affected by the LV blood pool.

B. Estimation of Relative Permittivity From Conductance (Admittance Magnitude) Measurements

Frequency-dependent resistivity measurements have been reported elsewhere [24]. These data are reanalyzed here to estimate the permittivity of cardiac muscle. From (3b), the magnitude of the admittance $|\psi_m|$ (in siemens per meter) can be expressed according to (6)

$$|\psi_m| = \sqrt{(\sigma_m)^2 + (\omega\epsilon_m)^2}. \quad (5)$$

To estimate the myocardial permittivity (ϵ_m), (5) can be rearranged:

$$\epsilon_m = \frac{\sqrt{|\psi_m|^2 - (\sigma_m)^2}}{\omega}. \quad (6)$$

At low frequencies, the $\omega\epsilon_m$ term in (5) is negligible and the measured admittance $\approx \sigma_m$, which was estimated from the reported resistivity at 1 kHz. This was substituted into (6) along

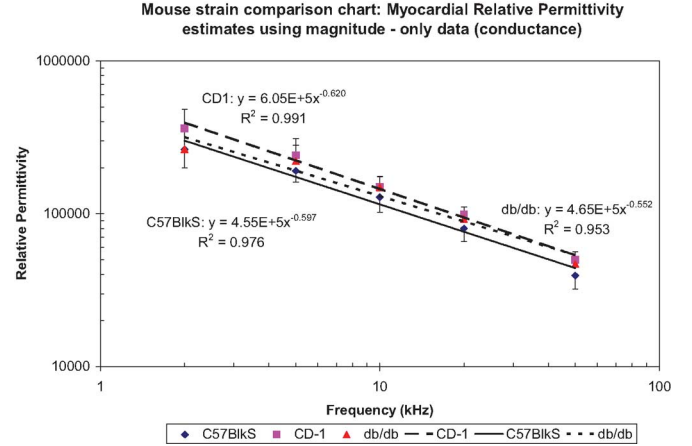


Fig. 6. Estimate of the relative permittivity of mouse LV myocardium from measurements of the magnitude of complex admittance (original data in [24]).

TABLE I
SUMMARY OF RELATIVE PERMITTIVITY ESTIMATES USING
MAGNITUDE-ONLY DATA

Frequency (kHz)	C57BlkS		db/db		CD-1	
	Mean	St. Dev.	Mean	St. Dev.	Mean	St. Dev.
2	263400	64400	264300	79500	362000	121500
5	190800	29800	221100	59100	241200	69300
10	128100	25700	149100	25400	149500	26400
20	80000	14500	92300	11000	98800	11800
50	39300	7070	46900	3870	49900	6380

with a higher frequency measurement of $|\psi_m|$ to obtain an estimate of ϵ_m .

The earlier calculations were performed on six randomly chosen mice ($N = 6$). The mean values are reasonably well-behaved and fit power curves quite closely (provided in Fig. 6). Table I summarizes the means and standard deviations at the different frequencies.

Repeated analysis of variance (ANOVA) statistical analysis using a $p = 0.05$ confidence interval was performed with three different *post hoc* comparison tests (Tukey honestly significant difference (HSD), least significant difference (LSD), and Bonferroni) to compare the relative permittivity estimates of the three different strains of mice: C57BlkS, db/db, and CD-1. The three different *post hoc* tests show high p -values ($p > 0.05$ in each case), indicating that the relative permittivity estimates from the three different strains of mice are not statistically different from each other. Since the estimated relative permittivities of these three strains of mice are not statistically different, we combined our prospective studies comparing magnitude-only (conductance), analog and digital studies on these different strains of mice.

C. Estimation of Myocardial Conductivity From Admittance Magnitude and Phase Measurements

When the surface probe is placed on the epicardium, the admittance measured is a combination of the contributions from the myocardium and the probe itself, so

$$Y_{\text{meas}} = Y_m + j\omega C_{\text{probe}} = G_m + j\omega C_m + j\omega C_{\text{probe}} \quad (7)$$

TABLE II
 MYOCARDIAL ELECTRICAL CONDUCTIVITY

Frequency (kHz)	Electrical Conductivity (S/m) (Digital Method) (N=10)		Electrical Conductivity (S/m) (Analog Method) (N=7)	
	Mean	Standard Deviation (%)	Mean	Standard Deviation (%)
2	0.160	0.099 (62)	0.142	0.043 (30)
5	0.166	0.095 (57)	0.150	0.046 (30)
10	0.176	0.103 (58)	0.154	0.046 (30)
20	0.175	0.106 (60)	0.159	0.046 (29)
50	0.169	0.109 (65)	0.179	0.043 (24)

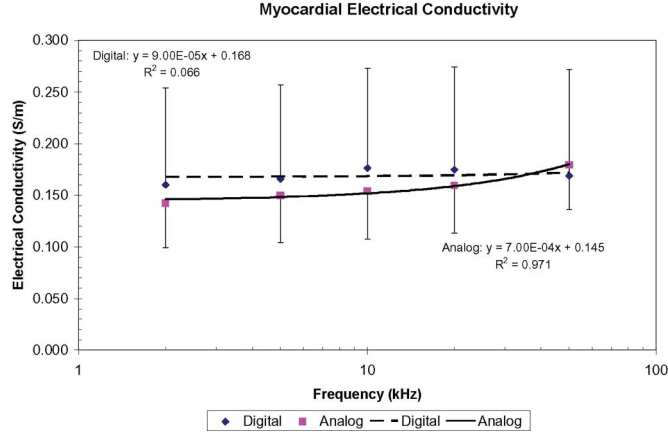


Fig. 7. Estimate of mouse-to-mouse variations in the electrical conductivity of mouse LV myocardium from the real part of the complex admittivity for CD-1 mice using the digital method ($N = 10$) and C57BlkS mice using the analog method ($N = 7$). Error bars are one standard deviation.

where Y_m is the admittance contribution from the myocardium and C_{probe} is the capacitance of the probe.

The real part of (7) yields the myocardial conductance (G_m , in siemens)

$$G_m = |Y_{\text{meas}}| \cos(\theta_{\text{meas}}) \quad (8a)$$

where $|Y_{\text{meas}}|$ is the measured admittance magnitude and θ_{meas} is the measured phase angle. The field form factor F is then estimated using known conductivity saline solutions. Then, using (2a) and (8a), the myocardial electrical conductivity is estimated (σ_m , in siemens per meter).

Table II lists the determination of myocardial electrical conductivity from admittance magnitude and phase measurements ($N = 10$ for digital method, $N = 7$ for analog method).

The individual mouse data mean values were combined to obtain the overall estimates across all mice. These values are plotted in Fig. 7 for both the digital and analog methods.

The slopes of the linear fits (presented in Fig. 7) are very small, indicating that the conductivity is essentially independent of frequency. Also, a repeated measures ANOVA between the digital and analog estimates of the electrical conductivity gave a $p = 0.772$ (for “between subjects” effects), indicating that the two sets of data are not statistically different from each other.

D. Estimation of Myocardial Relative Permittivity From Admittance Magnitude and Phase Measurements

Some of the imaginary part of (7) is due to the probe and wires. This can be estimated using the saline calibration curves

 TABLE III
 MYOCARDIAL RELATIVE PERMITTIVITY

Frequency (kHz)	Relative permittivity Conductance method		Relative permittivity:Complex		Relative permittivity:Complex plane analog	
	Mean	Std. Dev. (%)	Mean	Std. Dev. (%)	Mean	Std. Dev. (%)
2	362,000	121500 (34)	114,000	33500 (29)	80,600	25100 (31)
5	241,200	69300 (29)	47,500	13700 (29)	34,900	8000 (23)
10	149,500	26400 (18)	27,900	7170 (26)	20,300	3310 (16)
20	98,800	11800 (12)	14,900	4800 (32)	11,800	2690 (23)
50	49,900	6380 (13)	5,010	2680 (53)	4,970	2500 (50)

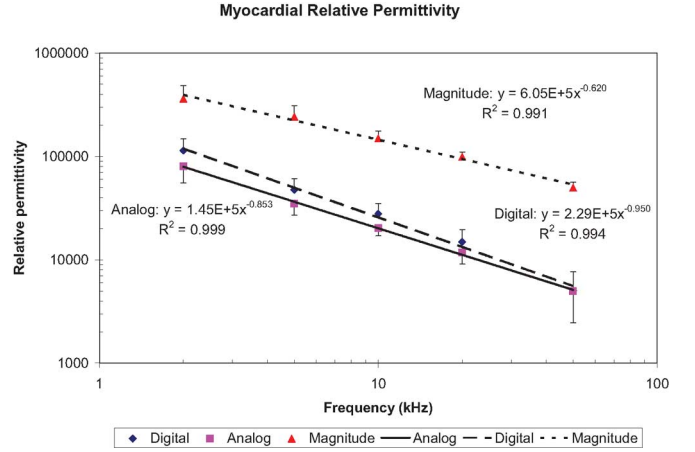


Fig. 8. Estimate of the mean relative permittivity of mouse LV myocardium from the imaginary part of the complex admittivity showing mouse-to-mouse variations. Combined data are for the same ten additional CD-1 mice as Fig. 7 for the digital method and the same seven additional C57BlkS mice as Fig. 7 for the analog method. Also shown is the estimation of relative permittivity from the magnitude-only (conductance) data from six randomly selected CD-1 mice. Error bars are one standard deviation.

(Fig. 4). Once compensated, the myocardial capacitance C_m (in farads) can be calculated from

$$C_m = \frac{|Y_{\text{meas}}| \sin(\theta_{\text{meas}}) - |Y_{\text{saline}}| \sin(\theta_{\text{saline}})}{\omega} \quad (8b)$$

where $|Y_{\text{meas}}|$ is the measured admittance magnitude and θ_{meas} is the measured phase angle, and $|Y_{\text{saline}}|$ is the interpolated (spline interpolation) admittance magnitude signal in saline and θ_{saline} is the interpolated (spline interpolation) phase signal in saline. The interpolation is done to estimate $|Y_{\text{saline}}|$ and θ_{saline} accurately in conductances in the vicinity of $|Y_{\text{meas}}|$, using the saline calibration curves generated in Section II-D of methods section. Finally, using (2b) and (8b), the myocardial permittivity ϵ_m (in farads per meter) is calculated.

Table III lists the estimates of myocardial relative permittivity (ϵ_r) from admittance magnitude ($N = 6$ CD-1 mice for conductance method), and both the complex admittance methods ($N = 10$ CD-1 mice for digital method and $N = 7$ C57BlkS mice for analog method).

The individual mouse data mean values were combined to obtain the overall estimates across all mice. These values are plotted in Fig. 8 for both the digital and the analog methods. Also shown, for comparison, is the estimation of relative permittivity from the magnitude-only data (conductance) on six randomly selected CD-1 mice.

The results show that the relative permittivity decreases with frequency in a logarithmic sense. Also, repeated measures

TABLE IV
REPEATED ANOVA ANALYSIS—*Post Hoc* RESULTS

Post - hoc method	Compare 1	Compare 2	p
Tukey HSD	Digital	Analog	0.606
LSD	Digital	Analog	0.345
Bonferroni	Digital	Analog	1
Tukey HSD	Digital	Magnitude	<0.0001
LSD	Digital	Magnitude	<0.0001
Bonferroni	Digital	Magnitude	<0.0001
Tukey HSD	Analog	Magnitude	<0.0001
LSD	Analog	Magnitude	<0.0001
Bonferroni	Analog	Magnitude	<0.0001

TABLE V
MURINE LV BLOOD ELECTRICAL CONDUCTIVITY

Frequency (kHz)	Electrical Conductivity (S/m)		Electrical Conductivity (S/m)	
	Mean	Std. Dev. (%)	Mean	Std. Dev. (%)
2	0.944	0.117 (12)	0.481	0.027 (6)
5	0.978	0.149 (15)	0.454	0.023 (5)
10	0.917	0.156 (17)	0.455	0.023 (5)
20	0.971	0.099 (10)	0.461	0.030 (7)
50	0.893	0.240 (27)	0.541	0.034 (6)

ANOVA with three different *post hoc* results indicate that the two complex measurements (the digital and analog approach) are not statistically different from each other ($p = 0.606$, $p = 0.345$, and $p = 1.0$). They also show that the magnitude-only (conductance) method estimates are statistically different from both the analog and digital methods. Table IV summarizes the *post hoc* results.

The magnitude-only (conductance) method has a large source of uncertainty at low frequencies arising from the subtraction of large numbers. This suggests that a complex measurement (both magnitude and phase of admittance) is more effective in estimating the electrical properties of the myocardium accurately than a magnitude-only (i.e., dual frequency) approach.

E. Estimation of Murine Blood Conductivity (With and Without Albumin Administration)

Murine blood electrical properties were measured on the same CD-1 mice with 0.4 mL of albumin administered during the course of the experiment ($N = 10$) and the same CBlk57S mice without albumin administration ($N = 7$). The imaginary component of the admittance (after catheter correction) was found to be negligible. Thus, all the conductivity estimates were performed using the real part of the admittance.

Table V lists the estimates of murine LV blood electrical conductivity from complex admittance. The individual mouse data mean values were combined to obtain the overall estimates across all mice. These values are plotted in Fig. 9 for both the mice with and without albumin administered during the experiment.

The results show that the blood conductivity does not vary with frequency. Also, the mean conductivity over all frequencies changes considerably with the administration of albumin (0.941 S/m with albumin and 0.478 S/m without albumin). Thus, albumin alters the blood conductivity by nearly 97%. Repeated

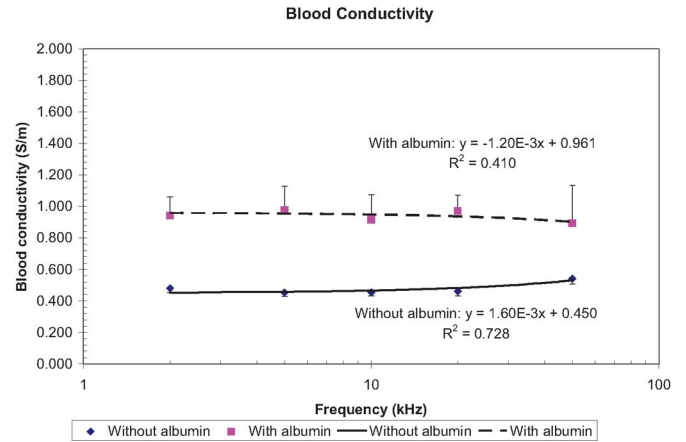


Fig. 9. Estimate of mouse-to-mouse variations in the electrical conductivity of mouse LV blood from the real part of the complex admittance for ten mice with albumin and seven mice without albumin. Error bars are one standard deviation.

measures ANOVA analysis generated a $p < 0.0001$, indicating that the two sets of data are statistically different from each other.

IV. DISCUSSION

A. Effect of Myocardial Anisotropy

The primary application for these results involves the measurement of P - V loops inside the murine LV using a tetrapolar catheter. The catheter measurement has contributions from both the blood and the myocardium. Myocardium is known to be highly anisotropic: the electrical conductivity in the longitudinal direction has been shown to be approximately twice that in the direction transverse to the fibers [15], [16]. Further, the fibers transition as much as 160° in the various “longitudinal planes” that make up the thickness of the myocardium, from epicardium to endocardium [30], [31]. Like the LV conductance catheter, the surface probe measurement is dominated by the longitudinal components; however, there is some contribution from the transverse direction. Our surface measurements in the mouse have been shown to be essentially insensitive to probe rotation relative to the longitudinal planes [24]. Some transverse/longitudinal anisotropy is always included in the lumped measurement provided by the surface probe. Needle electrodes, like the ones used by Salazar *et al.* [32] in their study of porcine myocardial tissue, would provide a longitudinal measurement alone; but needle electrodes are not practical in the extremely thin murine ventricular free wall due to the relative amount of tissue trauma they would cause.

B. Blood Conductivity Studies

The murine LV blood electrical conductivity means are higher than the means of electrical conductivities of LV myocardium. Mean myocardial conductivity σ_m ranged between 0.15 and 0.17 S/m while the mean blood conductivity was approximately 0.5 S/m without any albumin administered. Thus, we have verified experimentally that blood is approximately four times more conductive than myocardium. Further, over the frequencies used

TABLE VI
 $\omega\epsilon_m$ TERMS OBTAINED FROM DIGITAL PERMITTIVITY DATA

Frequency (kHz)	ϵ_r	$\omega\epsilon_m$
2	114,000	0.013
5	47,500	0.013
10	27,900	0.016
20	14,900	0.017
50	5,010	0.014

in this study, there was no measurable phase angle (after catheter effects correction) in blood. Thus, we can treat blood as a purely conductive medium. Finally, in a small animal, like a mouse, externally administered albumin (or similar electrolytes) significantly alters the electrical conductivity. This is a key point that researchers need to be aware of while performing murine LV catheter experiments.

C. Electrical Permittivity

Previously, Gabriel *et al.* [14] reported electrical permittivity values that range from approximately 200 000 at 2 kHz to about 20 000 at 50 kHz. They suggested that the high permittivity most likely originates in the cardiac myocyte transmembrane charge distribution. However, they had lumped the relative permittivity and conductivity into a complex permittivity. Salazar *et al.* [32] reported *in situ* complex resistivity measurements on porcine myocardium using needle electrodes. These data were reanalyzed to obtain the relative permittivity. The relative permittivity varied from about 190 000 at 2 kHz to about 23 000 at 50 kHz in their measurements, and the electrical conductivity was about 0.4 S/m. Our relative permittivity estimates varied from approximately 100 000 at 2 kHz to about 5000 at 50 kHz. Our epicardial surface probe measurements also include some transverse component, which accounts for the differences in the measurements. As discussed earlier, it is impractical for us to use needle electrodes on the murine myocardium due to the extremely thin nature of the ventricular free wall (approximately 1.2 mm at end systole and 0.8 mm at end diastole). We, however, suggest that since our goal is to determine the σ/ϵ ratio for the myocardium, our estimate of this ratio— 1.8×10^5 S/F at 2 kHz compared to Salazar *et al.* at 2.3×10^5 S/F—is useful for the intended purpose in spite of the limitation.

D. Choice of Optimal Frequency for LV P - V Experiments

We have observed that as the frequency increases, the relative permittivity decreases while the conductivity remains relatively constant. For further analysis, we calculated the $\omega\epsilon_m$ term [the imaginary component of the admittivity formulation in (3b)] at different frequencies (see Table VI).

The $\omega\epsilon_m$ term has a local maximum near 20 kHz, which is comparable to the measurements by Epstein and Foster [33]. This observation is a key point in the LV P - V analysis because this frequency will give the maximum resolvable imaginary cardiac muscle component.

E. Implications: Real-Time Parallel Myocardial Contribution Estimation and Removal in LV Volume Analysis

The complex measurement technique presented in this study is a progression of the initial formulation of Wei *et al.* [34] and can be used to estimate the electrical properties of myocardium in real time. The results of the current study have an important application during catheter-based LV P - V analysis in murine hearts, where the myocardial contribution to the measured admittance is changing instantaneously, and needs to be estimated and removed from the combined signal during the cardiac cycle. This is particularly important when transient occlusion of the inferior *vena cava* is performed to generate more complex measures of LV function available in the P - V plane such as end-systolic elastance, diastolic chamber compliance, and effective arterial elastance. Without true LV volume, absolute determination of these measures of ventricular function would not be available, but are desired by investigators of whole-heart mechanics.

The application of admittance to determine instantaneous LV volume allows comparison of measures of ventricular function between mice, and in a given mouse to itself over time. Current methods in determination of murine LV P - V suffer from a major limitation in that they fail to estimate a time-varying myocardial contribution within a heart cycle. However, this can be overcome by using real-time admittance that utilizes the capacitive component of muscle to remove the myocardium from the combined blood/myocardial signal, thus providing a broader application of this technology to invasive hemodynamic murine studies.

V. CONCLUSION

Complex admittance measuring instruments were designed and used to estimate the frequency-dependent myocardial electrical properties (conductivity and relative permittivity). The electrical conductivity was found to be essentially independent of the frequency of excitation. In contrast, the permittivity of myocardium was found to be inversely related to the frequency.

ACKNOWLEDGMENT

The authors would like to thank R. J. Treviño from The UTH-SCSA for his help with the murine experiments. They would also like to thank D. Altman for his help with the initial data collection and analysis.

REFERENCES

- [1] K. Sagawa, W. L. Maughan, H. Suga, and K. Sunagawa, *Cardiac Contraction and the Pressure-Volume Relationship*. New York: Oxford Univ. Press, 1988.
- [2] G. Esposito, L. F. Santana, K. Dilly, J. D. Santos Cruz, L. Mao, W. J. Lederer, and H. A. Rockman, "Cellular and functional defects in a mouse model of heart failure," *Amer. J. Physiol.: Heart Circ. Physiol.*, vol. 279, pp. H3101–H3112, 2000.
- [3] F. Franco, S. Dubois, R. M. Peschock, and R. V. Shohet, "Magnetic resonance imaging accurately estimates LV mass in a transgenic mouse model of cardiac hypertrophy," *Amer. J. Physiol.: Heart Circ. Physiol.*, vol. 274, pp. H679–H683, 1998.
- [4] F. Franco, G. D. Thomas, B. Giror, D. Bryant, M. C. Bullock, M. C. Chwialkowski, R. G. Victor, and R. M. Peschock, "Magnetic

- resonance imaging and invasive evaluation of development of heart failure in transgenic mice with myocardial expression of tumor necrosis factor- α ," *Circulation*, vol. 99, pp. 449–454, 1999.
- [5] M. D. Feldman, J. M. Erikson, Y. Mao, C. E. Korcarz, R. M. Lang, and G. L. Freeman, "Validation of a mouse conductance system to determine LV volume: Comparison to echocardiography and crystals," *Amer. J. Physiol.: Heart Circ. Physiol.*, vol. 274, pp. H1698–H1707, 2000.
- [6] J. Baan, T. T. Jong, P. L. Kerckhof, R. J. Moene, A. D. van Dijk, E. T. van der Velde, and J. Koops, "Continuous stroke volume and cardiac output from intraventricular dimensions obtained with impedance catheter," *Cardiovasc. Res.*, vol. 15, no. 6, pp. 328–334, Jun. 1981.
- [7] D. Georgakopoulos, W. A. Mitzner, C. H. Chen, B. J. Byrne, H. D. Millar, J. M. Hare, and D. A. Kass, "In vivo murine left ventricular pressure-volume relations by miniaturized conductance micromanometry," *Amer. J. Physiol.: Heart Circ. Physiol.*, vol. 274, pp. H1416–H1422, 1998.
- [8] B. Yang, J. Beishchel, D. F. Larson, R. Kelley, J. Shi, and R. R. Watson, "Validation of conductance catheter system for quantification of murine pressure-volume loops," *J. Invest. Surg.*, vol. 14, pp. 341–355, 2001.
- [9] E. B. Lankford, D. A. Kass, W. L. Maughan, and A. A. Shoukas, "Does volume catheter parallel conductance vary during a cardiac cycle?," *Amer. J. Physiol.: Heart Circ. Physiol.*, vol. 258, no. 6 (pt. 2), pp. H1933–H1942, Jun. 1990.
- [10] P. A. White, C. I. O. Brooks, H. B. Ravn, E. E. Stenbøg, T. D. Christensen, R. R. Chaturvedi, K. Sorensen, V. E. Hjortdal, and A. N. Redington, "The effect of changing excitation frequency on parallel conductance in different sized hearts," *Cardiovasc. Res.*, vol. 38, pp. 668–675, 1998.
- [11] T. J. Gawne, K. S. Gray, and R. E. Goldstein, "Estimated left ventricular offset volume using dual-frequency conductance technology," *J. Appl. Physiol.*, vol. 63, pp. 872–876, 1987.
- [12] D. Georgakopoulos and D. A. Kass, "Estimation of parallel conductance by dual-frequency conductance catheter in mice," *Amer. J. Physiol.: Heart Circ. Physiol.*, vol. 279, pp. H443–H450, 2000.
- [13] S. Gabriel, R. W. Lau, and C. Gabriel, "The dielectric properties of biological tissues: II. Measurements in the frequency range 10 Hz to 20 GHz," *Phys. Med. Biol.*, vol. 41, no. 11, pp. 2251–2269, 1996.
- [14] S. Gabriel, R. W. Lau, and C. Gabriel, "The dielectric properties of biological tissues: III. Parametric models for the dielectric spectrum of tissues," *Phys. Med. Biol.*, vol. 41, no. 11, pp. 2271–2293, 1996.
- [15] P. Steendijk, G. Mur, E. van der Velde, and J. Baan, "The four-electrode resistivity technique in anisotropic media: Theoretical analysis and application on myocardial tissue in vivo," *IEEE Trans. Biomed. Eng.*, vol. 40, no. 11, pp. 1138–1148, Nov. 1993.
- [16] S. Rush, J. A. Abildskov, and R. McFee, "Resistivity of body tissues at low frequencies," *Circulation Res.*, vol. 12, pp. 40–50, 1963.
- [17] H. P. Schwan and C. F. Kay, "Specific resistance of body tissues," *Circulation Res.*, vol. 4, pp. 664–670, 1956.
- [18] N. Sperelakis and G. Sfyris, "Impedance analysis applicable to cardiac muscle and smooth muscle bundles," *IEEE Trans. Biomed. Eng.*, vol. 38, no. 10, pp. 1010–1022, Oct. 1991.
- [19] P. Steendijk, E. van der Velde, and J. Bann, "Dependence of anisotropic myocardial electrical resistivity on cardiac phase and excitation frequency," *Basic Res. Cardiol.*, vol. 89, pp. 411–426, 1994.
- [20] J.-Z. Tsai, J. A. Will, S. Hubard-van Stelle, H. Cao, S. Tungjitkusolmun, Y. B. Choy, D. Haemmerich, V. R. Vorperian, and J. G. Webster, "In vivo measurement of swine myocardial resistivity," *IEEE Trans. Biomed. Eng.*, vol. 49, no. 5, pp. 472–483, May 2002.
- [21] J.-Z. Tsai, J. A. Will, S. Hubard-van Stelle, H. Cao, S. Tungjitkusolmun, Y. B. Choy, D. Haemmerich, V. R. Vorperian, and J. G. Webster, "Error analysis of tissue resistivity measurement," *IEEE Trans. Biomed. Eng.*, vol. 49, no. 5, pp. 484–494, May 2002.
- [22] P. M. Edic, G. J. Saulnier, J. C. Newell, and D. Isaacson, "A real-time electrical impedance tomography," *IEEE Trans. Biomed. Eng.*, vol. 42, no. 9, pp. 849–859, Sep. 1995.
- [23] L. Borcea, "Electrical impedance tomography," *Inverse Problems*, vol. 18, pp. R99–R136, 2002.
- [24] M. Reyes, M. Steinhilper, J. Alvarez, D. Escobedo, J. A. Pearce, J. W. Valvano, B. Pollock, C.-L. Wei, A. T. G. Kottam, D. Altman, S. Lee, S. Bailey, S. L. Thomsen, G. Freeman, and M. D. Feldman, "Impact of physiologic variables and genetic background on myocardial frequency-resistivity relations in the intact beating murine heart," *Amer. J. Physiol.: Heart Circ. Physiol.*, vol. 291, no. 4, pp. H1659–H1669, Oct. 2006.
- [25] A. Kottam and J. Pearce, "Electric field penetration depth of myocardial surface catheters and the measurement of myocardial resistivity," *Biomed. Sci. Instrum.*, vol. 40, pp. 155–160, 2004.
- [26] A. Kottam, "Determination of parasitic circuit elements in cardiac conductance catheters," M.S. thesis, Dept. Biomed. Eng., Univ. Texas at Austin, Austin, 2003.
- [27] K. Raghavan, "A real-time approach towards in vivo phase measurements for the determination of volume in the murine heart," M.S. thesis, Dept. Electr. Comput. Eng., Univ. Texas at Austin, Austin, 2004.
- [28] K. Raghavan, C. L. Wei, A. Kottam, D. G. Altman, D. J. Fernandez, M. Reyes, J. W. Valvano, M. D. Feldman, and J. A. Pearce, "Design of instrumentation and data-acquisition system for complex admittance measurement," *Biomed. Sci. Instrum.*, vol. 40, pp. 453–457, 2004.
- [29] A. Kottam, "Measurement of electrical admittance to study the onset and progression of myocardial ischemia," Ph.D. dissertation, Dept. Biomed. Eng., Univ. Texas at Austin, Austin, 2007.
- [30] D. D. Streeter, S. M. Spotnitz, D. P. Patel, J. Ross, Jr., and E. H. Sonnenblick, "Fiber orientation in the canine left ventricle during diastole and systole," *Circ. Res.*, vol. 24, pp. 339–347, 1969.
- [31] D. D. Streeter and W. T. Hanna, "Engineering mechanics for successive states in canine left ventricular myocardium," *Circ. Res.*, vol. 33, pp. 656–664, 1973.
- [32] Y. Salazar, R. Bragos, O. Casas, J. Cinca, and J. Rosell, "Transmural versus nontransmural in situ electrical impedance spectrum for healthy, ischemic, and healed myocardium," *IEEE Trans. Biomed. Eng.*, vol. 51, no. 8, pp. 1421–1427, Aug. 2004.
- [33] B. R. Epstein and K. R. Foster, "Anisotropy in the dielectric properties of skeletal muscle," *Med. Biol. Eng. Comput.*, vol. 21, pp. 51–55, Jan. 1983.
- [34] C. L. Wei, J. W. Valvano, M. D. Feldman, M. Nahrendorf, R. Peshock, and J. A. Pearce, "Volume catheter parallel conductance varies between end-systole and end-diastole," *IEEE Trans. Biomed. Eng.*, vol. 54, no. 8, pp. 1480–1489, Aug. 2007.



Karthik Raghavan received the B.E. (Hons.) degree in electronics and instrumentation engineering from Birla Institute of Technology and Science, Pilani, India, in 2002, and the M.S.E. degree in electrical and computer engineering in 2004 from The University of Texas at Austin, Austin, where he is currently working toward the Ph.D. degree in electrical and computer engineering.



John E. Porterfield received the B.S. degree in electrical engineering from Oklahoma State University, Stillwater, in 2004, and the M.S.E. degree in electrical and computer engineering in 2006 from The University of Texas at Austin, Austin, where he is currently working toward the Ph.D. degree in electrical and computer engineering.

His current research interests include biomedical instrumentation, bioimpedance measurement, and computer modeling.



Anil T. G. Kottam received the B.Tech. degree in biomedical engineering from Cochin University of Science and Technology, Kochi, India, in 2001, and the M.S.E. and Ph.D. degrees in biomedical engineering from The University of Texas at Austin, Austin, in 2003 and 2007, respectively.

He is currently a Research Engineer at Scisense, Inc., London, ON, Canada.



Marc D. Feldman received the B.S. degree from Duke University, Durham, NC, in 1977, and the M.D. degree from the University of Pennsylvania School of Medicine, Philadelphia, in 1981.

He completed his internship and residency at Billings Hospital, University of Chicago, Chicago, IL. He was a Clinical and a Research Fellow in cardiology at Beth Israel Hospital, Harvard Medical School, Boston, MA. He is currently a Professor of medicine and engineering, and the Director of the Cardiac Catheterization Laboratories, Division of

Cardiology, The University of Texas Health Sciences Center at San Antonio, San Antonio. He is also an Adjunct Professor at The University of Texas at Austin, Austin.



Jonathan W. Valvano (M'83) was born in Clinton, CT, in 1953. He received the B.S. degree in computer science and engineering and the M.S. degree in electrical engineering and computer science from Massachusetts Institute of Technology (MIT), Cambridge, in 1977, and the Ph.D. degree in medical engineering from Harvard University/MIT Division of Health Sciences and Technology, Cambridge, in 1981.

He is currently a Full Professor at The University of Texas at Austin, Austin, where he is engaged in research in the fields of perfusion measurements, bioinstrumentation, and bioheat transfer models.



Daniel Escobedo is a self-taught very experienced animal surgeon affiliated with The University of Texas Health Sciences Center at San Antonio (UTH-SCSA), San Antonio.

He is a Research Associate in the Department of Medicine/Cardiology, The University of Texas Health Sciences Center at San Antonio. He has over 25 years of experience with animal surgery with expertise in microsurgery in rodents. He has also been a consultant for Millar Instruments and Scisense, Inc. He is a coauthor of 12 published papers.



John A. Pearce (S'79–M'80–SM'92) received the B.S.M.E. and the M.S.M.E. degrees from Clemson University, Clemson, SC, in 1968 and 1971, respectively, and the M.S.E.E. and Ph.D. degrees in electrical engineering from Purdue University, West Lafayette, IN, in 1977 and 1980, respectively.

In 1982, he joined the Faculty of Electrical and Computer Engineering, The University of Texas at Austin, Austin, where he is currently the Department Undergraduate Adviser and the Adviser for the Biomedical Engineering Track in the Graduate Program. His current research interests include interactions between electromagnetic fields and tissues. He is also involved in the basic science of "electrosurgery," and the application of RF current to cut and coagulate tissues. He is currently investigating how the complex electrical properties of cardiac muscle can be applied to identify its contribution to the electrical admittance signal.

Dr. Pearce won the Presidential Young Investigator Award from the National Science Foundation in 1985.